



Title	AN INVESTIGATION OF THE MECHANISM OF THE HYDROGEN ELECTRODE PROCESS ON A MERCURY CATHODE AT HIGH ELECTRODE POTENTIAL
Author(s)	MITUYA, Atusi
Citation	JOURNAL OF THE RESEARCH INSTITUTE FOR CATALYSIS HOKKAIDO UNIVERSITY, 4(3), 228-255
Issue Date	1957-03
Doc URL	http://hdl.handle.net/2115/24653
Type	bulletin (article)
File Information	4(3)_P228-255.pdf



[Instructions for use](#)

AN INVESTIGATION OF THE MECHANISM OF THE HYDROGEN ELECTRODE PROCESS ON A MERCURY CATHODE AT HIGH ELECTRODE POTENTIAL

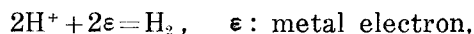
By

Atusi MITUYA^{*)}

(Received February 25, 1957)

Introduction

It is the well-known empirical relationship found by TAFEL that the logarithm of current density i of the hydrogen electrode reaction



varies linearly with the electrode potential η of the cathode referred to the reversible hydrogen electrode as

$$\log i = -\alpha F\eta/RT + \text{constant}, \quad 0 < \alpha < 1.$$

BOWDEN and RIDEAL,¹⁾ with their exhaustive studies confirmed this relationship for numerous metal electrodes. That α is a proper fraction and moreover a constant near $\frac{1}{2}$ independent of η for most of hydrogen electrodes, has drawn attention of a number of investigators and they have tried to find out a common mechanism, which accounts for this conspicuous aspect of the hydrogen electrode reaction.

HORIUTI and OKAMOTO²⁾ found that the separation factors of heavy hydrogen for various metal electrodes at 0.3 volt cathodic polarization at room temperature were distinctly divided into two groups i.e. 6 to 7 for cathodes of Pt, Ni, Au, Ag, Cu, Fe, and Pb (alkaline), and 3 to 4 for those of Hg, Sn, and Pb (acid). Recognizing as did by TOPLEY and EYRING,³⁾ that the separation factor depends only on the rate determining step, they have attributed the catalytic mechanism, controlled by the recombination of chemisorbed hydrogen atoms to the former group and the electrochemical mechanism governed by the neutrali-

^{*)} Chemical Laboratory, St. Paul's University, Tokyo.

zation of chemisorbed hydrogen molecule-ion to the latter group*).

OKAMOTO, HORIUTI and HIROTA^{d)} have actually calculated the separation factor statistical-mechanically in agreement with the observed value with reference to nickel of the former group of the hydrogen electrodes. HORIUTI, KEII and HIROTA^{e)} have on the other hand worked out the separation factor on the basis of the electrochemical mechanism with special reference to mercury cathode in concordance with the observation. The TAFEL rule that α remains constant near $\frac{1}{2}$ has also been accounted for on the basis of the respective mechanism. It has been, moreover, predicted from the catalytic mechanism that α reduces to 2 or 0 according as η is sufficiently high or low outside the observed region of η , whereas from the electrochemical mechanism that α is near $1\frac{1}{2}$ or $\frac{1}{2}$ according as η is high or low but never reduces to zero over the region where the reverse current is negligible.

The slow discharge mechanism has on the other hand revealed itself more or less attractive with regard to the explanation of α being constant near $\frac{1}{2}$, in so far as one remains with the classical kinetics assumed to be valid to the elementary reaction on the electrode surface; as well known, TAFEL has thus obtained 2 instead of observed $\frac{1}{2}$ on the basis of the catalytic mechanism. HORIUTI *et al.*^{d), e)} have explained that α is a constant near $\frac{1}{2}$ on the very basis of the catalytic mechanism but taking the repulsive interaction of chemisorbed hydrogen atoms, which causes an appreciable deviation from the classical kinetics.

It is the purpose of the present work further to investigate the mechanism of the hydrogen electrode reaction on mercury. Among three mechanisms mentioned above, the catalytic mechanism may be excluded at the outset, since the energy of two hydrogen atoms chemisorbed on mercury electrode is nearly as high as two free hydrogen atoms, as inferred from the minute dissociation energy of HgH (0.37eV), so that no observable reaction could ever take place through this state. Our procedure of investigation was now to check the theoretical predictions deduced from the electrochemical mechanism by experiments

*^{d)} According to the original statement of the mechanism, it was the act of formation of hydrogen molecule from a chemisorbed hydrogen atom H(a), a proton H⁺, and a metal electron ϵ , which governed the rate of the electrode process; i. e. H⁺ + H(a) + ϵ → H₂. The present expression, H₂(a) + ϵ → H₂, was adopted, since it has turned out later by an actual calculation that the electronic state of H and H⁺ before the neutralization was such as adequately covered by words "hydrogen molecule-ion adsorbed on the electrode". Cf. Ref. 5.

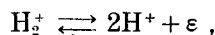
comparatively with those from the slow discharge mechanism.

The electrochemical mechanism predicts now, as mentioned above, that the TAFEL constant α lies near $1\frac{1}{2}$ or $\frac{1}{2}$ according as electrode potential η is high or low. The increase of TAFEL constant by one at higher electrode potential is caused according to the electrochemical mechanism as follows. The probability of a single hydrogen molecule-ion to discharge is proportional to $\exp(-\alpha_0 F\eta/RT)$ where α_0 is a constant near $\frac{1}{2}$.⁵⁾ The chemical potential of chemisorbed hydrogen molecule-ion μ^{H_2} or that of metal electron μ^ϵ is expressed^{7)*)} as,

$$\begin{aligned}\mu^{\text{H}_2^+} &= RT \log (\theta/1-\theta) - RT \log q_0^{\text{H}_2^+} + u \\ \mu^\epsilon &= -F\eta + \text{constant},\end{aligned}$$

where θ is the probability that a site σ for H_2^+ is occupied by the latter, $-RT \log q_0^{\text{H}_2^+}$ the reversible work required to bring up a hydrogen molecule-ion onto the site σ from the reference state in the absence of the interaction with surrounding adsorptives and u the part of the work due to the latter interaction.

On account of the preliminary equilibrium



we have

$$\mu^{\text{H}_2^+} = 2\mu^{\text{H}^+} + \mu^\epsilon$$

and hence

$$RT \log (\theta/1-\theta) + u = -F\eta + \text{constant}^{**}).$$

*) According Eqs. (8.14) and (5.1) of Ref. 8 we have

$$\mu^{\text{H}_2^+} = RT \log \theta_{\sigma(\text{H}_2^+)}/\theta_{\sigma(\epsilon)} - RT \log q_\sigma^{\text{H}_2^+},$$

where $\theta_{\sigma(\text{H}_2^+)}$ or $\theta_{\sigma(\epsilon)}$ is the probability that the site σ of adsorption is occupied by

H_2^+ or none respectively and $-RT \log q_\sigma^{\text{H}_2^+}$ is the reversible work required to bring up H_2^+ from its reference state onto σ . Rewriting $\theta_{\sigma(\text{H}_2^+)}$ into θ and $\theta_{\sigma(\epsilon)}$ into $1-\theta$, neglecting the probability of adsorption of other adsorptives in accordance with the result of Ref. 5 we have the equations in the text, dividing the work $-RT \log q_\sigma^{\text{H}_2^+}$

further into two parts, $-RT \log q_0^{\text{H}_2^+}$ and u . Cf. § 27, Ref. 7.

***) The work $-RT \log q_0^{\text{H}_2^+}$ is constant at constant temperature according to the definition.

As u is of the repulsive interaction⁵⁾, it increases with θ and hence θ decreases according to the above relation with increasing η . When θ is sufficiently small that u practically vanishes, θ or the population of chemisorbed hydrogen molecule-ion is proportional to $\exp(-F\eta/RT)$. The current is now proportional at this condition to $\exp(-(1+\alpha_0)F\eta/RT)$ or the TAFEL constant, $\alpha = -\frac{RT}{F} \frac{\partial \log i}{\partial \eta}$, is $1+\alpha_0$.

When θ attains a certain value with decreasing η , the increase of u with θ becomes remarkable, so that the further increase of θ with decreasing η is appreciably checked and practically completely when θ is close to unity. At this stage α practically equals α_0 as observed.

We consider now the charge E to be supplied along with the creation of new electrode surface at constant η . As the repulsive interactions between hydrogen molecule-ions sets in to reduce the value of α from $1+\alpha_0$ to α_0 , the rate of increase of E with decreasing η , or the capacity of the electrode surface must be simultaneously reduced, because of the increase of H_2^+ is checked by the repulsive interaction and that of H^+ also, as the latter is repulsed by H_2^+ too as shown by the detailed calculation of HORIUTI, KEII and HIROTA⁵⁾.

On the basis of slow discharge mechanism on the other hand, there is no reason why α should change and the capacity should too, hydrogen atoms formed by the rate-determining slow discharge step being practically in equilibrium with hydrogen gas at constant pressure leaving the electrode surface invariable with respect to their adsorption.

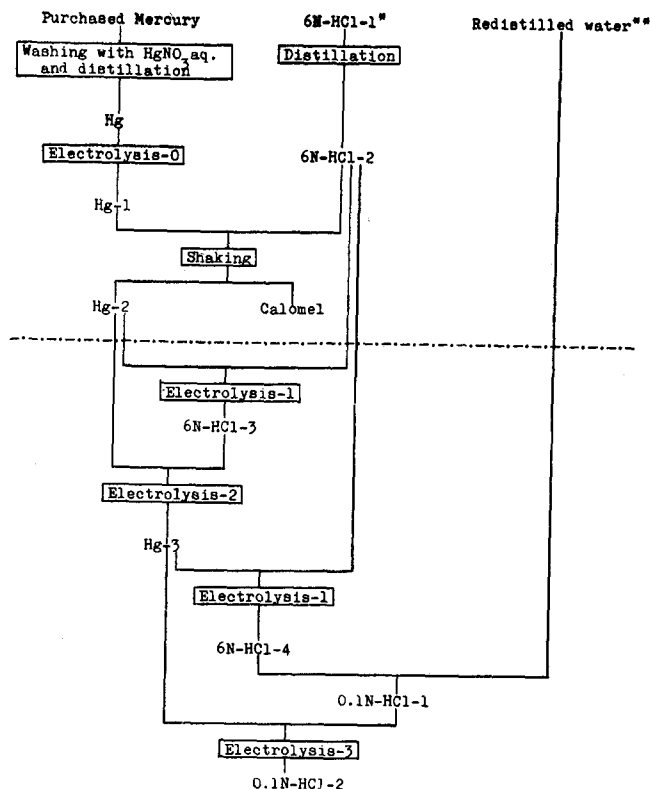
We are thus able to discriminate between the electrochemical and the slow discharge mechanism by observing i - η -relation as well as E - η -relation simultaneously.

Present author has previously⁵⁾ measured i - η -relation finding actually the transition of α from $1+\alpha_0$ to α_0 . In the present work the latter observation was carried out in conjunction with that of the E - η -relation respectively at conditions adjusted as close as possible to each other with appreciably improved degree of purity of electrodes as well as of electrolyte as described below.

§ 1. Materials

(1) Mercury and 0.1N-HCl

Mercury for the electrode and 0.1 N-HCl for the electrolyte were prepared from purchased mercury and 6 N-HCl formed from synthe-



*cf. §1 - (1)

**cf. §1 - (2)

Diagram 1 Schematic Diagram of purification

sized 12N-HCl, 36N-H₂SO₄ for analysis and redistilled water*) by procedures shown in the Diagram 1 above.

Lines there show the flow of materials through individual procedure of purifications indicated in rims, combination or branching of the lines showing the two kinds of materials getting into or coming out from the procedure of purification. Hg-1, Hg-2, etc. show materials in progressing degree of purification. The horizontal chain line shows that the procedures above or below it were conducted in air or in vacuum respectively.

6N-HCl-1 was prepared as follows. The 36N-H₂SO₄ for analysis was dropped into the synthesized 12N-HCl at 50°C. The liberated

*) Cf. (2). Redistilled water used in the present work is all of the same preparation.

hydrogen chloride was introduced into redistilled water to make a solution of 6N-HCl. This solution was distilled in an all glass apparatus in air to prepare 6N-HCl-1.

Purchased mercury was purified as shown in the Diagram ordinarily by washing with aqueous solution of mercuric nitrate and distilled in air, successively by Electrolysis-0, shaking with 6N-HCl-2, Electrolysis-1 and -2 down to Hg-3; Electrolysis-0 is the electrolysis of 2N-HNO₃ with mercury to be purified as anode and platinum as cathode in air after BRUMMER and NARAY-SZÁBÓ⁽¹⁾ followed by wash with redistilled water. Electrolysis-1 is that of 6N-HCl between mercury and platinum as cathode and anode respectively in vacuum and Electrolysis-2 is the electrolysis using the very 6N-HCl purified by Electrolysis-1, with two mercury electrodes in vacuum. The anode mercury thus purified is Hg-3.

Electrolysis-1 is illustrated in Fig. 1.

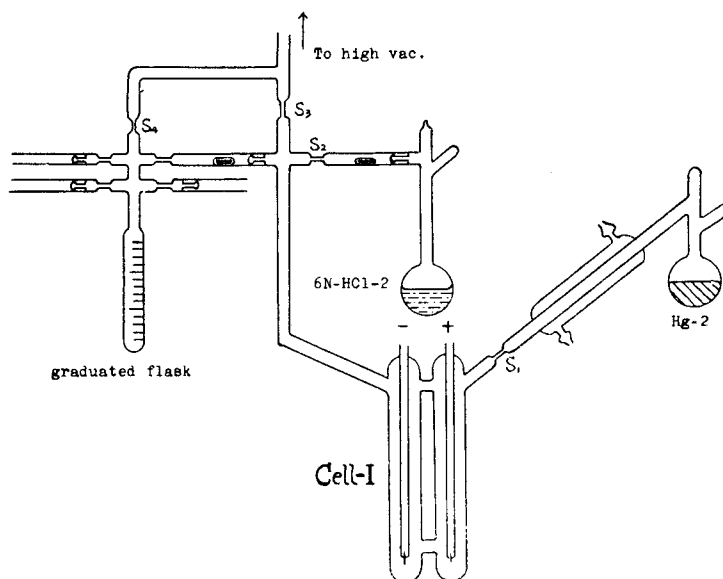


Fig. 1 Illustration for Electrolysis-1 to make 6N-HCl-3.

Hg-2 was distilled in vacuum without boiling into the right branch of the electrolytic cell, Cell-I, leaving the left branch empty and the constriction S₁ was sealed off. 6N-HCl-2 sealed in vacuum in a flask was now distilled without boiling into Cell-I and the constriction S was sealed off. After Electrolysis-1 was carried out in Cell-I between

mercury and platinum as cathode and anode, the content was frozen by liquid air and evacuated for removing the gas evolved by the electrolysis; this procedure was repeated four times to make sure the removal. The 6N-HCl in Cell-I was distilled into a graduated flask to prepare 6N-HCl-3 and the constrictions S_3 and S_4 were sealed off.

Fig. 2 shows the Electrolysis-2 for the preparation of Hg-3; Hg-2 so far purified in air was now sealed in a evacuated flask and distilled

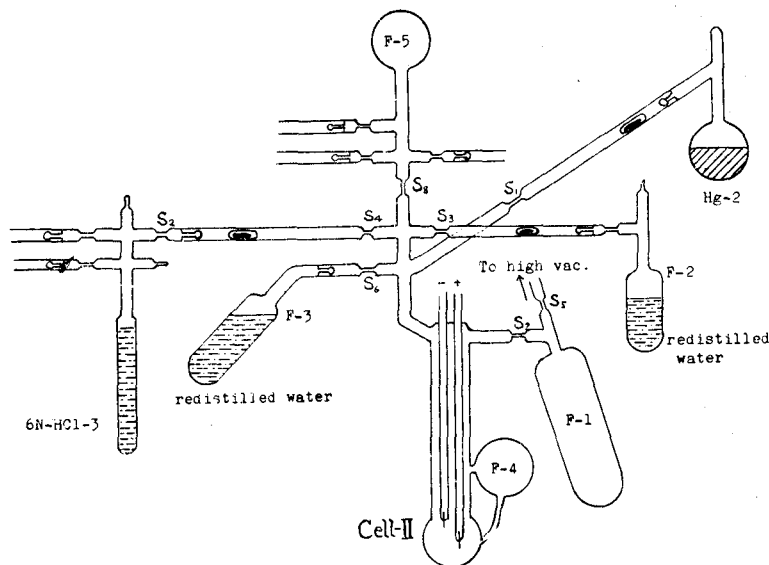


Fig. 2 Illustration for Electrolysis-2 to make Hg-3.

into Cell-II just to cover the lower tip of platinum contact and the constriction S_1 was sealed off. A portion of 6N-HCl-3 prepared in the graduated flask as above was now distilled into Cell-II and then redistilled water sealed in vacuum in Flask 2 was added to the distillate by distillation to make 2N-HCl and to cover the higher platinum tip of Cell-II. After constrictions S_2 , S_3 , S_4 and S_5 were sealed off, 2N-HCl in Cell-II was electrolysed between the mercury anode and the platinum cathode for 24 hours. The electrolyte was now decanted into the Flask 1 using Flask 4 as the mercury trap. Flask 3 was now communicated to Cell-II and redistilled water, sealed in vacuum in Flask 3 with its axis in a plane perpendicular to the plane of the figure, was decanted into Cell-II for washing mercury there; the wash was drained into

Flask 1 and after this procedures of washing were repeated several times, constrictions S_6 and S_7 were sealed off and one of joints of Flask 5 was fused to the vacuum line, communicated to the latter to evacuate the whole apparatus. The apparatus was now sealed off at the joint, and mercury in the Cell-II was finally decanted into Flask 5 to prepare Hg-3 in Flask 5*^o) by sealing S_8 off.

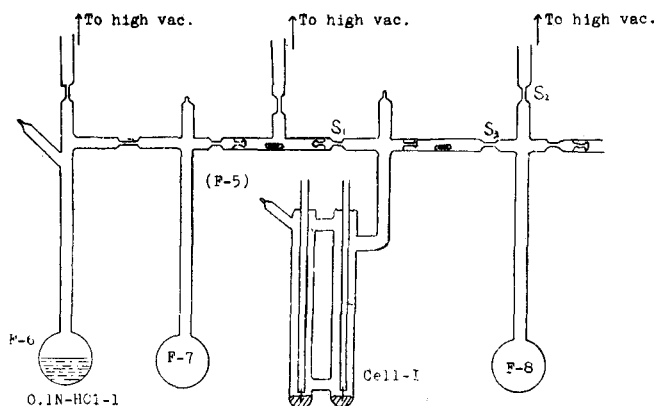


Fig. 3 Illustration for Electrolysis-3 to make 0.1N-HCl-2.

Tenth normal hydrochloric acid, 0.1N-HCl-1 in F-6, was prepared from 6N-HCl-2 by electrolyzing it with Hg-3 as cathode and platinum as anode i. e. by Electrolysis-1 similarly as that shown in Fig. 1, and by diluting the resultant electrolyte 6N-HCl-4 by redistilled water, distilling the dilution into F-6. A proper quantity of Hg-3 in F-5 was preliminarily distilled into the Cell-I of Fig. 1 to provide mercury electrodes as shown in the figure and then F-5 was sealed off. The hydrochloric acid in F-6 was now distilled into F-7 and then F-6 was sealed off. After the interspace between F-7 and Cell-I was evacuated and sealed off from the vacuum line, the 0.1N-HCl-1 was distilled from F-7 into Cell-I and S_1 was sealed off. The 0.1N-HCl-1 was now electrolysed for 30 hours. After the gas evolved by the electrolysis was removed by repeating the evacuation of the frozen electrolyte as described above with reference to Electrolysis-1, S_2 was sealed off and 0.1N-HCl thus purified was distilled into F-8 and S_3 was sealed off to finish the final electrolyte 0.1N-HCl-2 sealed in vacuum.

The all electrolytic treatments referred to above were terminated

*^o) Hereinafter all flasks numbered as Flask 5, 6, etc. will be described as F-5, F-6, etc.

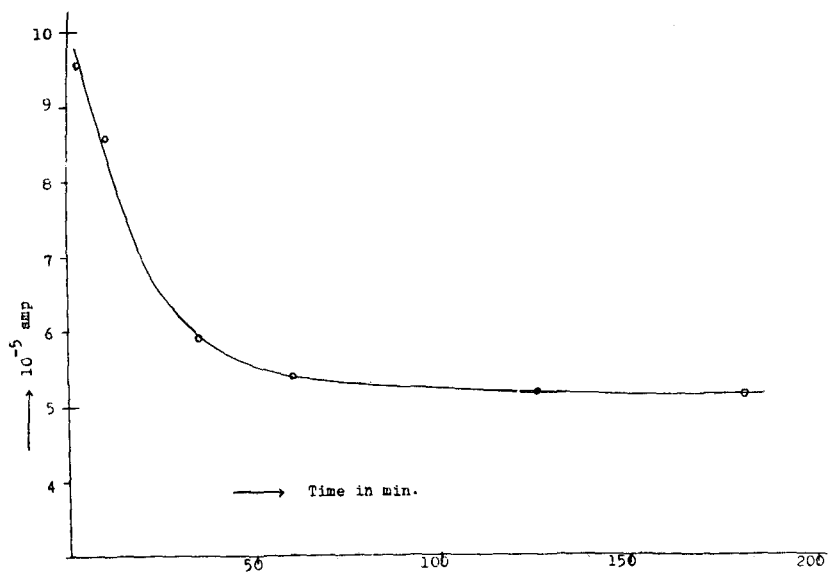


Fig. 4 Change of current density with time. Electrolysis-1 of 6N-HCl-3 with Hg-anode and Pt-cathode, terminal potential 607 mV, 23°C.

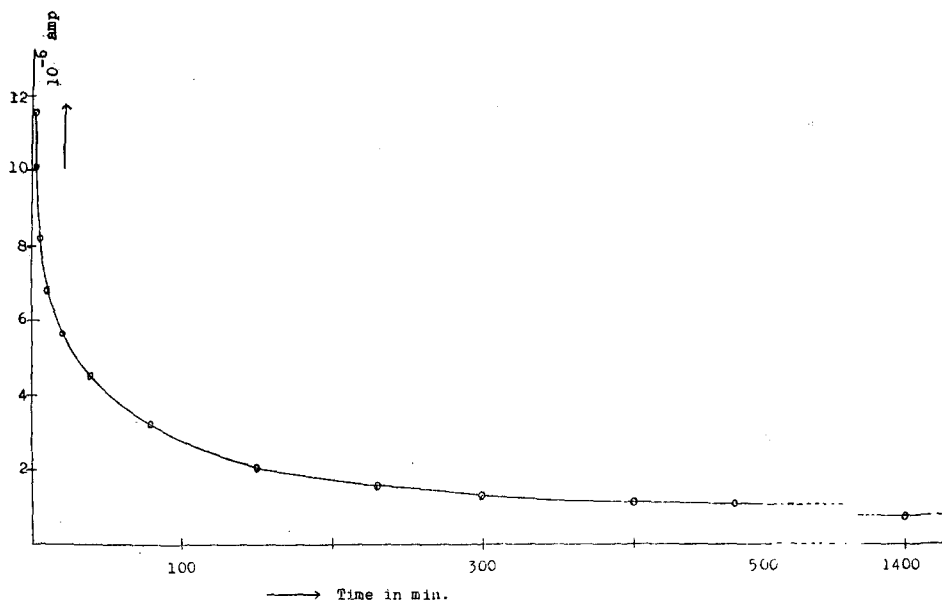


Fig. 5 Change of current density with time. Electrolysis-2 of Hg-3 with Hg-electrodes, terminal potential 616 mV, 19°C.

according to AZZAM, BOCKRIS, CONWAY and ROSENBERG,¹⁰⁾ at the stage when the electrolytic current attained a constant value after about 24–30 hours. The results of Electrolysis-1, -2 and -3 are shown in Figs. 4, 5, and 6 respectively.

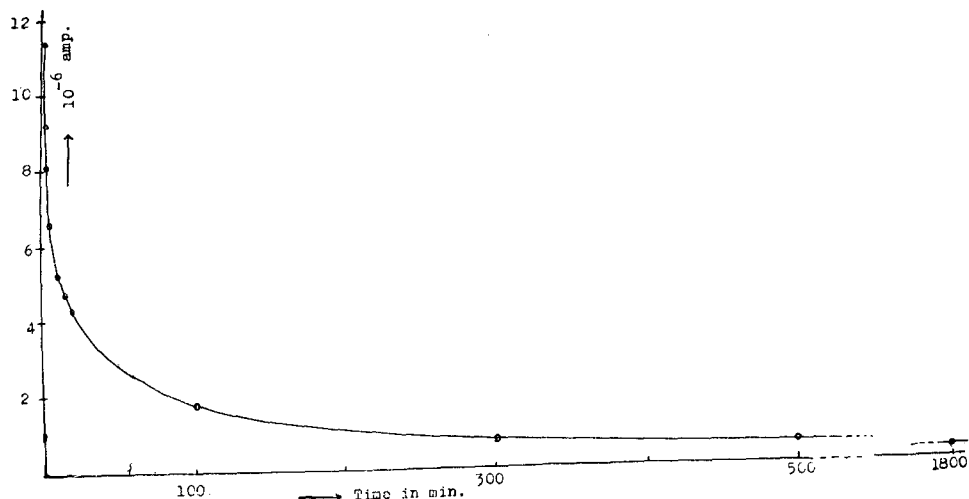


Fig. 6 Change of current density with time.
Electrolysis-3 of 0.1N-HCl-2 with Hg-electrodes,
terminal potential 616 mV, 20°C.

Mercury-3 and 0.1N-HCl-2 were used for the determination of $\log i-\eta$ -and of $E-\eta$ -relations.

(2) **Redistilled water**

Tap water was passed through a monobed column filled with ion exchange resins, added with KMnO_4 and NaOH , and distilled in an all-glass system. The distillate was redistilled in another all-glass system, and was kept in a quartz flask.

(3) **Platinum**

Platinum for the anode and the reference electrode was platinum wire of 0.08–0.1mm diameter guaranteed by the dealer, TANAKA Precious Metal Work Co. Tokio, as 99.99% as determined by spectral analysis.

(4) **Hydrogen**

Hydrogen was electrolytically prepared from a solution of NaOH for analysis in redistilled water, dried over silica gel, passed through

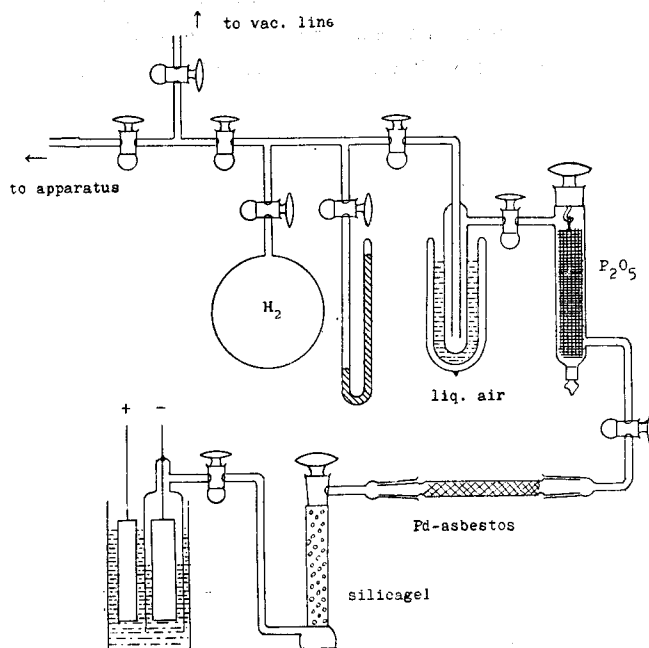


Fig. 7 Preparation and purification of hydrogen.

a tube packed with about 50 cm long palladium-impregnated asbestos kept at 350°C, over P_2O_5 and then through a trap in liquid air, and stored in a 3 litre flask H_2 , shown in Fig. 7.

§ 2. The cell for determining $\log i-\eta$ -relation

Fig. 8 shows the Cell-A, used for the determination of the $\log i-\eta$ -relation, which was designed to fulfil the following requirements:

- (1) The cell must be charged with purified electrolyte and mercury, i.e., 0.1N-HCl-2 and Hg-3, without exposing them to air.
- (2) The part of the cell containing the electrolyte must be of the simplest possible geometry so that the current due to the mercury electrode reaction is readily eliminated by partially establishing an equilibrium with respect to the latter as mentioned later in §5.

This cell was provided with a platinum anode, a platinum reference electrode, and a mercury cathode and charged with 0.1N-HCl solution and hydrogen gas at about 76 cmHg pressure. Cell-A was prepared and charged with the contents as follows. Glass tubes of suitable

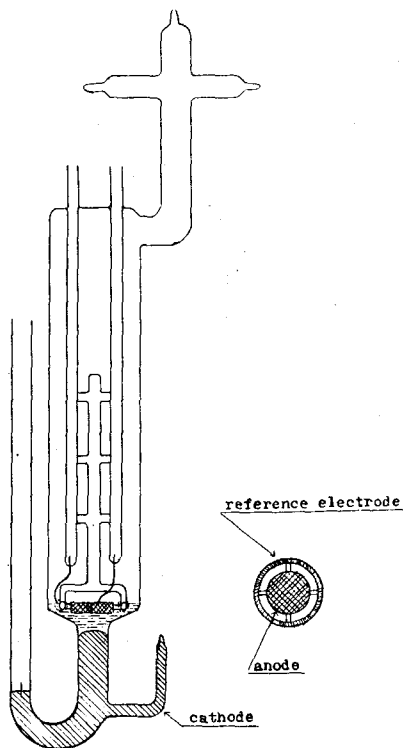


Fig. 8 Cell-A.

size, made of borosilicate glass (a sort of Pyrex glass) were flushed with a solution of 20% hydrofluoric acid, washed thoroughly with hot water, 6N-HNO₃ solution, hot water and distilled water. Then they were worked up to form a cell shown in Fig. 9, provided with a platinum anode, a reference electrode, and platinum electric contact P for a mercury cathode. Then the cell was washed with 2N-HF solution for five minutes, distilled water, distilled 6N-HNO₃ solution, distilled water, 6N-HCl-1, distilled water and hot redistilled water, and finally dried *in vacuo*.

Platinum anode was a disk of about 3 cm in diameter formed by folding platinum gauze of about 300 cm² in area, which was mounted in the cell with a glass-sealed leads, as was shown in Fig. 8.

Reference electrode was platinum wire of 0.08 mm diameter wound on a glass ring mounted around the anode.

The procedures of charging the cell are as follows.

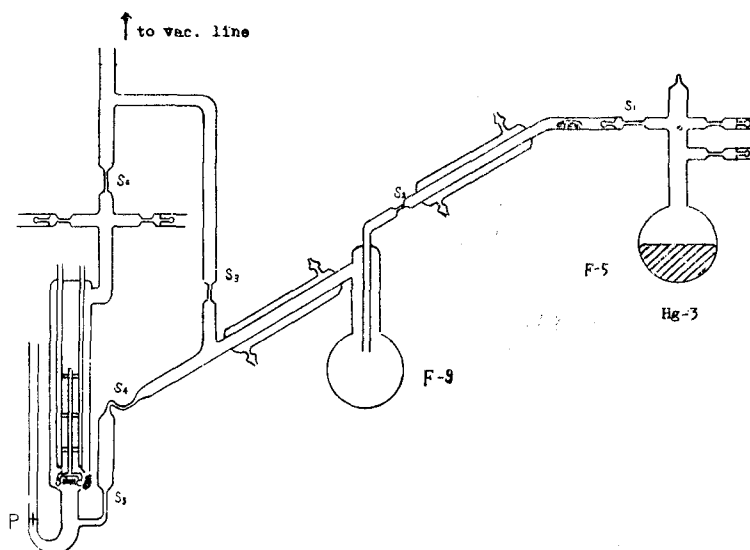


Fig. 9 Introduction of purified Hg-3 into the cell

(1) Introduction of mercury into the cathode compartment of the cell.

The flask F-5, in which Hg-3 was stored, was attached to the cooler as shown in Fig. 9 and the whole apparatus shown there was fused to the vacuum line *via* mercury stop and a liquid oxygen trap and evacuated to 10^{-7} mmHg; F-9 there was then gradually heated up to 300°C , while the evacuation still continued. The pressure increased at the beginning of the heating and then decreased; the latter procedure of heating and evacuation was continued until the pressure decreased down to approximately 10^{-5} mmHg. The necessary amount of mercury for Cell-A was now distilled from F-5 into F-9 with evacuation still continued and then the flask F-5 and the cooler were sealed off at S_1 and S_2 . F-9 was cooled by dry ice-methanol bath during the distillation to avoid the contamination of platinum electrodes by mercury vapour. Now vessels on the lefthand side of S_2 in Fig. 9 were evacuated to 10^{-7} mmHg. The cell was now heated at 300°C in an electric furnace leaving F-9 still in the above bath under the continued evacuation and the remaining parts were heated with a burner flame. After whole the system was cooled to room temperature, a small amount of purified hydrogen was introduced and then evacuated repeatedly with an intention of washing out other gases adsorbed on the glass wall. Finally, the cell was cooled to -20°C , and the mercury was distilled into the

cell from F-9 by removing the dry ice-methanol bath and heating the flask by a hand burner; and then hydrogen gas was admitted into the cell, to prevent any further contamination of the platinum electrodes by mercury vapour. After that the remaining constrictions S_2 , S_4 , S_5 and S_6 were all sealed off.

(2) Introduction of 0.1N-HCl-solution into the cell.

Now F-8 containing 0.1N-HCl-2 was fused to a joint of the cell as shown in Fig. 10 and hydrogen gas in the cell was evacuated from S_2 without opening F-8 and then S_2 sealed off.

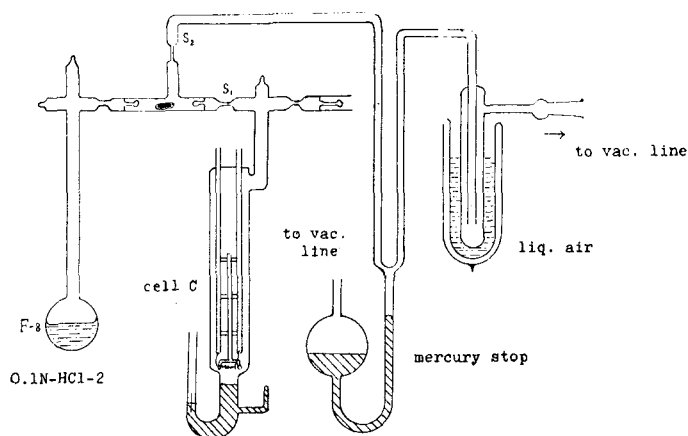


Fig. 10 Introduction of 0.1N-HCl-2 to the cell.

The cell kept at -20°C , was now communicated to F-8 to distill 0.1N-HCl-2 in it gently without boiling into the cell so much as just to wet the platinum anode and the reference electrode for facilitating both the platinum electrodes to work reversibly under hydrogen gas above.

(3) Introduction of hydrogen gas.

After the electrolyte was introduced into the cell the constriction S_1 was sealed off and the cell was connected to the vacuum line by the remaining joint. After a proper evacuation purified hydrogen kept in a flask H_2^* was expanded carefully through a liquid oxygen trap into the cell kept at 0°C to 70.3 cmHg pressure. Cell-A is now finished by sealing off the constriction of the last joint.

*) Cf. §1-(4) and Fig. 7.

§ 3. The cell for determining $E-\eta$ -relation

With the purpose stated in the introduction, the $E-\eta$ -relation was observed, using the same preparations of purified electrolyte and mercury, at experimental conditions adjusted as close as possible to that of the measurement of $\log i-\eta$ -relation.

Fig. 11 shows Cell-B, the apparatus used for the experiment, which is of the same structure and content as that of Cell-A except that mercury electrode is contained in a U-tube, instead of in a blind tube, the mercury meniscus in one of its branch serving as the electrode in contact with the solution, that the cell is attached with an additional chamber C_1 , which is connected with the other branch of the U-tube to make a circuit and that the anode and the reference electrode is platinum wires of 0.08 mm diameter wound as shown in the Figure around the radial glass frame fixed inside the chamber C_2 .

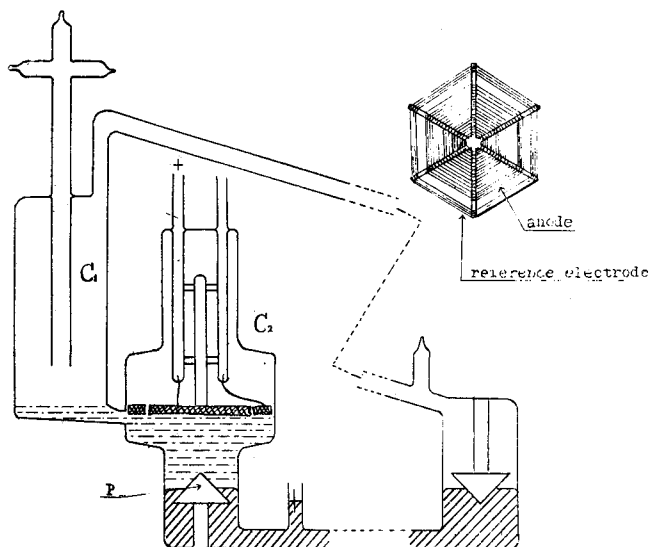


Fig. 11 Scheme of Cell-B.

The horizontal part of the U-tube is 40 cm long and of 10 mm diameter. Both the vertical branches of it are of 37 mm diameter fitted in it with a pair of rectangular prisms of the same form fixed invertedly to each other.

The chamber C_1 is about 300 cc. volume, the gas phase in the chamber C_2 180 cc and the electrolyte phase in C_2 26 cc.

The procedure of charging Cell-B with 0.1N-HCl-2 and Hg-3 is quite similar to that of Cell-A.

Mercury was so much admitted into Cell-B as both the mercury meniscuses rest, at a proper inclination of the U-tube, just at the middle height between the vertex and the base of the respective prisms.

The Cell-B rest on a knife edge fixed beneath P and its rightward end could be driven upwards by means of a plunger rod of a piston pressed out by oil at constant rate; the oil was pressed in at a constant rate by another piston with its plunger rod screwed in by means of a synchronous motor. The inclination of Cell-B was thus varied at constant rate within 2°. The constant rate of the variation of inclination was changed by a pulley system attached to the synchronous motor.

In this way the area of the electrode in contact with the solution could be varied at a constant rate as shown below. Let h_l or S_l be the height above the horizontal part of the U-tube or the area of the mercury meniscus respectively in the left branch of the U-tube and h_r or S_r that in the right branch. We have for the variation of the area dS_l or dS_r , caused by that of inclination

$$dS_l = a \cdot dh_l, \quad dS_r = -a \cdot dh_r \quad (1. l), (1. r),$$

since the prisms are of the same form and placed invertedly to each other, where $a (>0)$ is a constant particular to the geometry of prisms and dh_l or dh_r , the increment of the height of the meniscus caused by the increment of the inclination. We have however because of the incompressibility of mercury

$$S_l \cdot dh_l + S_r \cdot dh_r = 0,$$

or eliminating dh_l and dh_r from the above three equations,

$$S_l \cdot dS_l = S_r \cdot dS_r$$

or by integration

$$S_l^2 = S_r^2 + \text{const.}$$

The integration constant is however zero, inasmuch as the mercury level was adjusted to pass through the middle height of both the prisms at a particular inclination, when $S_l = S_r$. It follows that

$$S_l = S_r \quad (2)$$

throughout.

But since the inclination of Cell-B is varied at constant rate, the difference h_i-h_r of the heights referred to Cell-B must also be varied at constant rate, say C , i. e.

$$d(h_i-h_r) = C \cdot dt$$

where t is time. Eliminating dh_i and dh_r from (1.1), (1.7) and the above equation, we have now

$$dS_i + dS_r = a \cdot C \cdot dt$$

or according to (2)

$$dS_i/dt = \frac{1}{2} a \cdot C$$

i. e. the rate of the variation of the electrode surface S_i is a constant.

§ 4. Experimental procedure

Diagram 2 and 3 show the circuit for Cell-A and Cell-B respectively.

Battery B, in Diagram 3 applies a desired potential between anode and cathode of Cell-B through the ballistic galvanometer G of 755 Ω internal resistance by means of the potentiometric divider circuit. Battery B, there is used for eliminating a constant electrolytic current i through G with another potentiometric divider circuit switched in three steps by means of the switch S, according to the order of magnitude of the constant current to be eliminated. C is a capacity of 50 μ F, which is charged by a 200 V potential source of 0.1% constancy; the

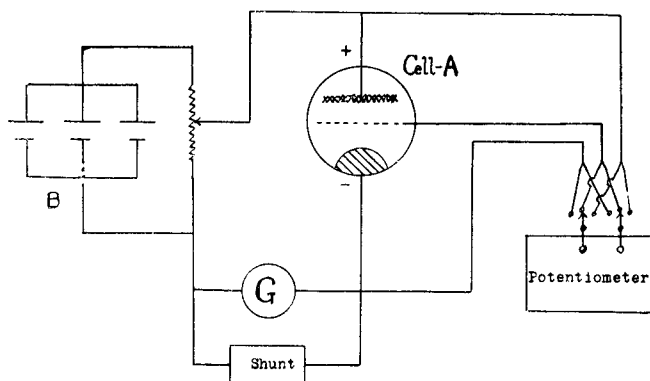
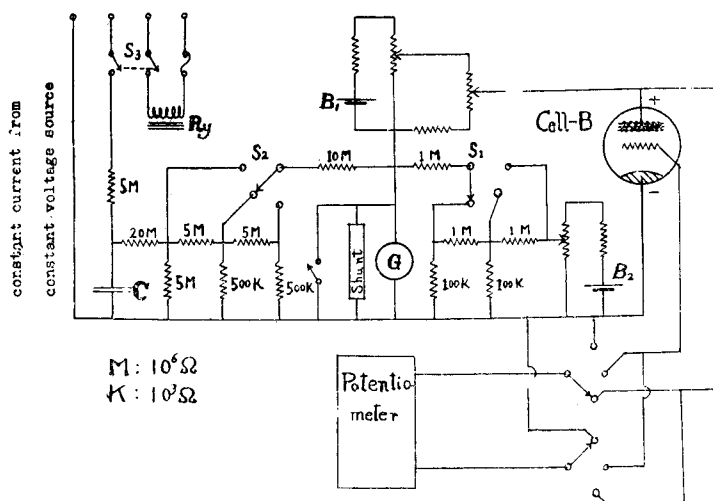


Diagram 2 Circuit for Cell-A.



linear part of about 120 V range was used by means of the potentiometric divider circuit with the three steps switch S_2 similar to the above one for eliminating the increase of the electrolytic current proportional to the electrode surface. R_y is the relay switch to start the synchronous motor for steadily changing the inclination of Cell-B; R_y is operated simultaneously with the charging of the capacity C.

The observations with Cell-A are conducted as follows. The potential difference between the anode and the reference electrode is measured at first without setting in the current between the platinum anode and the mercury cathode to make sure that the reference electrode as well as the anode are working as reversible hydrogen electrodes. Potential of a definite magnitude is now applied between the anode and the cathode by means of the potentiometric divider circuit following the current by a galvanometer. From time to time the potential between the anode and the reference electrode was measured by means of the switches at the potentiometer to make sure that the anodic polarization remained within 0.6 mV. The current was found monotonously to decrease down to a steady value particular to the magnitude of the potential applied. This trend was accounted for, as described later, as an approach to the partial equilibrium with respect to the mercury electrode reaction. On the basis of this explanation the steady current finally attained was taken as that due to the hydrogen electrode reaction.

After the first measurement of the steady current described above, the potential applied was shifted to another fixed value to observe the steady current finally attained. The potential was thus changed from a fixed value to another successively observing the final steady current for each fixed potential. The current was found to increase or decrease according as the previous fixed potential is smaller or greater in absolute magnitude than the present one. This effect being similarly explained as an approach to the partial equilibrium with respect to the mercury electrode reaction, the steady current finally attained was taken similarly as that due to the hydrogen electrode reaction.

The observation of $E-\eta$ -relation by means of Cell-B was conducted as follows. Similarly as in the case of Cell-A, it was ascertained that the potential difference between the anode and the reference electrode was tolerably small and then that the current at any definite potential of the mercury cathode was just similarly attained as in the case of Cell-A. The circuit for eliminating this steady current i was now switched on, adjusting the deflection of the galvanometer to the null-point on the scale. The cathode surface area was now increased at a constant rate dS/dt by switching on S_3 and the charging-up current was directly measured by G by compensating the part due to the hydrogen electrode reaction iS , which increases at a constant rate idS/dt , by the capacity C with the potentiometric divider circuit.

The compensation current was adjusted as follows; dS/dt was determined by measuring the time for varying the inclination by a definite amount by a stop watch on one hand and by measuring the associating variation of the height of the mercury meniscus relative to the prism by means of a cathetometer on the other hand; the latter measurement and the known geometry of the prism gives the increase of the surface area and hence dS/dt . The compensation current is now $i \cdot \frac{ds}{dt} \cdot t$ and the potential to be applied to the terminals of G to effect the latter current is now $i \frac{ds}{dt} \cdot t \cdot R$, where R is the internal resistance of G; the latter potential is applied by C adjusting the potentiometric divider circuit by preliminary calculation.

§ 5. Result

(1) Change of current density with time and $\log i-\eta$ -relation.

The current density was found, as stated above, at a fixed potential

of the mercury cathode to decrease or increase asymptotically to a definite value accordingly as the cathode potential was lowered or raised from the former fixed potential, after an initial very large current momentarily increasing or decreasing similarly. Attributing this large current to the charging or discharging of the double-layer, it is possible to determine its capacity by measuring the amounts of electricity charged or discharged, by the throwing angle method using a ballistic galvanometer, although the determination was not carried out in the present work.

It was concluded from the above experimental facts that the observed current consists, besides of the charging or discharging current of the capacity, of the current of the hydrogen evolution and that of mercury dissolution, and that our closed cell of simple geometry favoured the latter side reaction prevailing to attain, at a definite polarisation in the present experiment, to its own equilibrium state, automatically adjusting, along with the time, the mercury ion concentration. The final steady current was taken, in consequence, as that of the genuine hydrogen electrode reaction.

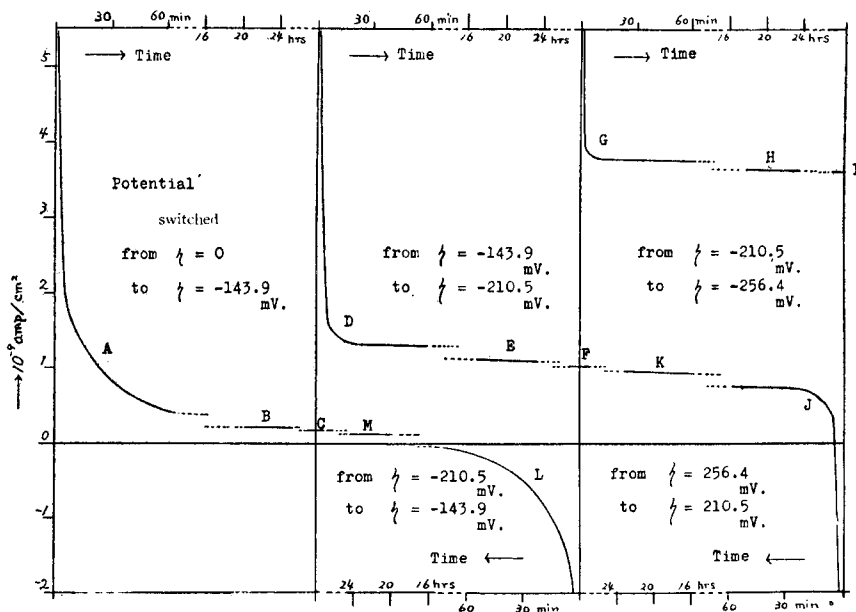


Fig. 12 Changes of current density with time, when the potential switched from a definite constant value to another.

The current density-time relationships thus observed are shown in Fig. 12.

As the cathode was first cathodically polarised by 143.9 mV from zero potential, the current followed the curve A as far as 60 min from the moment of the polarisation. The segment B of the curve shows the current around 24 hrs after the moment of the initial polarization. Forty hours later than the moment, the current was found to assume a value shown by the point C; when the potential was lowered to a new value -210.5 mV, the current varied initially as shown by the curve D, around 24 hrs as E, and then settled after 40 hrs at the point F; when the potential further decreased to a new constant value, -256.4 mV, the current varied similarly as curves G and H, settling again after 40 hrs at I; when the potential was increased to the former value -210.5 mV, the current suddenly decreased even inverting its sign initially and then gradually increased as shown by the curve J, and around 24 hrs as K, settling after 40 hrs at F, i. e. just at the steady value attained previously by lowering the potential stepwise. Curves L and M show the variation of the current as the potential finally switched to the initial value, i. e. -143.9 mV, reproducing 40 hrs after the switch the point C formerly attained.

The asymptotic value of the current at a definite potential was thus quite reproducible, irrespective of the history of the cathode potential.

It was found, moreover, that the polarization of the platinum anodes of Cell-A and Cell-B against the respective reference electrode were always less than 6×10^{-4} volt at current densities up to 10^{-8} amp in the present experiments.

The cathodic current density i directly observed is now generally related with the forward and backward current \bar{I} and \tilde{I} as

$$i = \bar{I} - \tilde{I} \quad \text{and} \quad i = \bar{I} \left(1 - e^{-\frac{\nu k \eta}{RT}} \right)$$

according to HORIUTI and IKUSIMA¹¹⁾ and HORIUTI⁷⁾ where ν is the stoichiometric number of the rate-determining step. As the cathode potential η was at least -120.5 mV, the exponential term in the parenthesis is negligible compared with unity, whether ν be 1 or 2, i. e. the observed i is practically identical with \bar{I} or the reverse current \tilde{I} is negligible as mentioned in the introduction as proviso with reference to the theoretical prediction.

The results obtained by Cell-A at 0°C is shown in Fig. 13 and in

Table I.

TABLE I. Current density of hydrogen electrode reaction

Cell-A, 0°C

Area of the mercury cathode: 0.25 cm²
 Area of the platinum anode: 300 cm²
 Pressure of hydrogen gas: 75.0 cm Hg at 23°C

η in mV	$i = \bar{i}$ in Amp	$\log i$
- 176.6	2.09×10^{-9}	9.320
- 131.7	7.56×10^{-10}	10.879
- 96.1	7.41×10^{-11}	11.870
- 148.2	1.07×10^{-9}	9.029
- 159.2	1.47×10^{-9}	9.168
- 171.1	1.98×10^{-9}	9.296
- 200.0	3.74×10^{-9}	9.573
- 219.6	5.44×10^{-9}	9.736
- 110.0	1.84×10^{-10}	10.265
- 118.0	3.80×10^{-10}	10.580

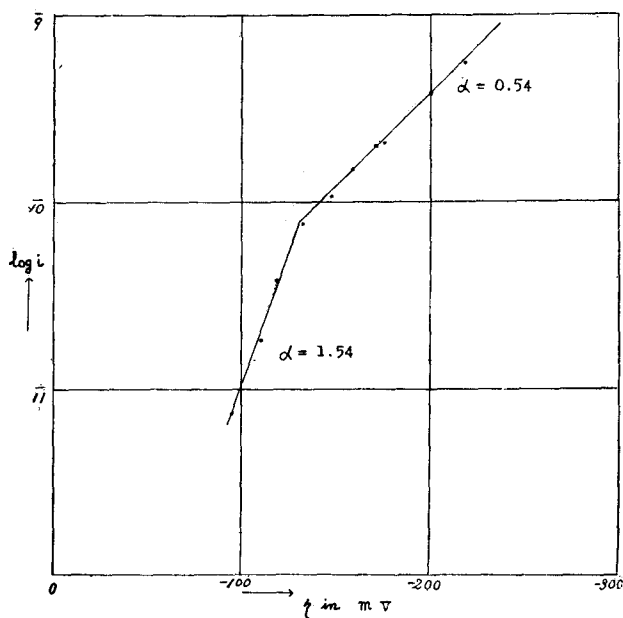


Fig. 13 The $\log i-\eta$ -relation observed by Cell-A.

We see clearly from Fig. 13 that there exists distinctly a break on the $\log i-\eta$ curve just as previously observed.⁸⁾ The α value is derived from the parts of the curve at potentials respectively below or above that of the break as 0.54 or 1.54 respectively.

Similar series of experiments have also been carried out with Cell-B before the measurements of charging up currents with similar results as shown in Fig. 14 and Table II.

TABLE II. Current density of hydrogen electrode reaction

Cell-B

Area of the mercury cathode: 10.5 cm²
 Area of the platinum anode: 100 cm²
 Pressure of hydrogen gas: 75.5 cm Hg at 18°C

Temperature	η in mV	$i = \bar{i}$ in amp
0 °C	- 143.9	1.35×10^{-10}
	- 210.5	1.01×10^{-9}
	- 256.4	3.60×10^{-9}
	- 375.6	7.20×10^{-8}
	- 401.2	1.09×10^{-7}
	- 319.5	1.65×10^{-8}
	- 167.1	4.22×10^{-10}
	- 121.8	0.60×10^{-10}
	- 157.6	3.99×10^{-10}
	- 356.9	3.70×10^{-8}
	- 144.8	1.64×10^{-10}
	- 166.5	4.20×10^{-10}
- 154.3	3.00×10^{-10}	
12 °C	- 143.9	2.24×10^{-10}
	- 210.5	1.52×10^{-9}
	- 255.4	5.05×10^{-9}
	- 317.5	3.30×10^{-8}
	- 379.1	1.36×10^{-7}
	- 359.8	6.70×10^{-8}
	- 274.8	1.24×10^{-8}
	- 166.5	8.90×10^{-10}
	- 144.3	3.51×10^{-10}
	- 181.8	9.34×10^{-10}
	- 227.9	3.89×10^{-9}
	- 144.9	3.78×10^{-10}
- 120.5	0.70×10^{-11}	

An Investigation of the Mechanism of the Hydrogen Electrode Process

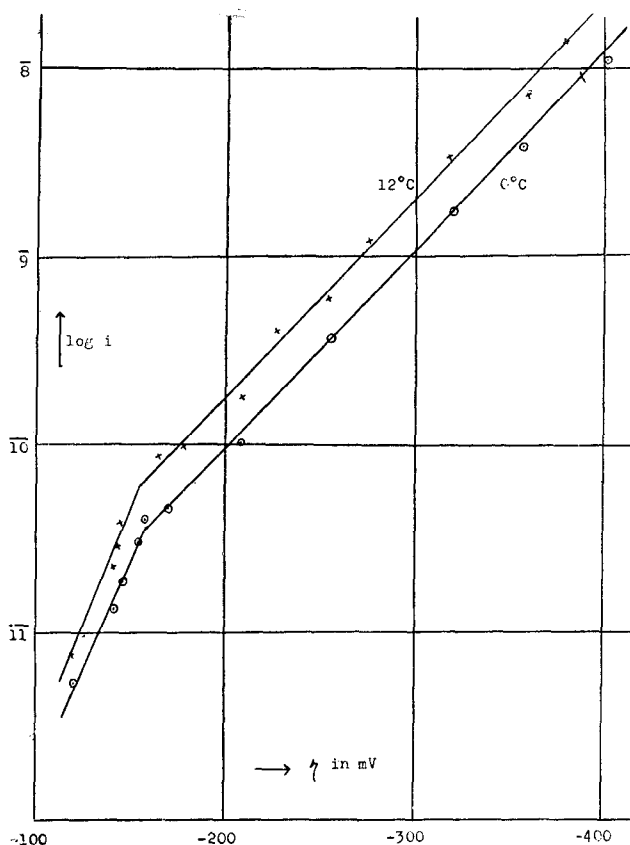


Fig. 14 The $\log i - \eta$ -relation observed by Cell-B.

The potential of the break at 0°C observed with Cell-B is different from that with Cell-A but they are brought to coincidence by taking the difference of the potential of the reference electrode into account, i. e., by reducing the potential of the former by $\frac{RT}{2F} \log \frac{P_B C_A}{P_A C_B}$ where P_A and P_B is the hydrogen pressure and C_A and C_B is the concentration of hydrogen ion in Cell-A and in Cell-B respectively.

Figs. 13 and 14 show that the experimental results fit exclusively in with the conclusion derived from the electrochemical mechanism stated in the introduction.

(2) **Result of the measurement of $E-\eta$ -relation.**

The observed charging up current divided by the rate dS/dt of

increase of the cathode area gives the electricity E , and E divided by electronic charge e gives the number of charges E' required to form unit cathode area, which is shown in Fig. 15.

As shown in the Figure the capacity or the inclination of the curve is smaller at lower electrode potential and the change from the larger to the smaller inclination occurs just at the "break" of $\log i-\eta$ curve, in confirmation of the conclusions derived from the electrochemical mechanism mentioned in the introduction. It is concluded that the only possible mechanism of the hydrogen electrode reaction on mercury cathode is the electrochemical.

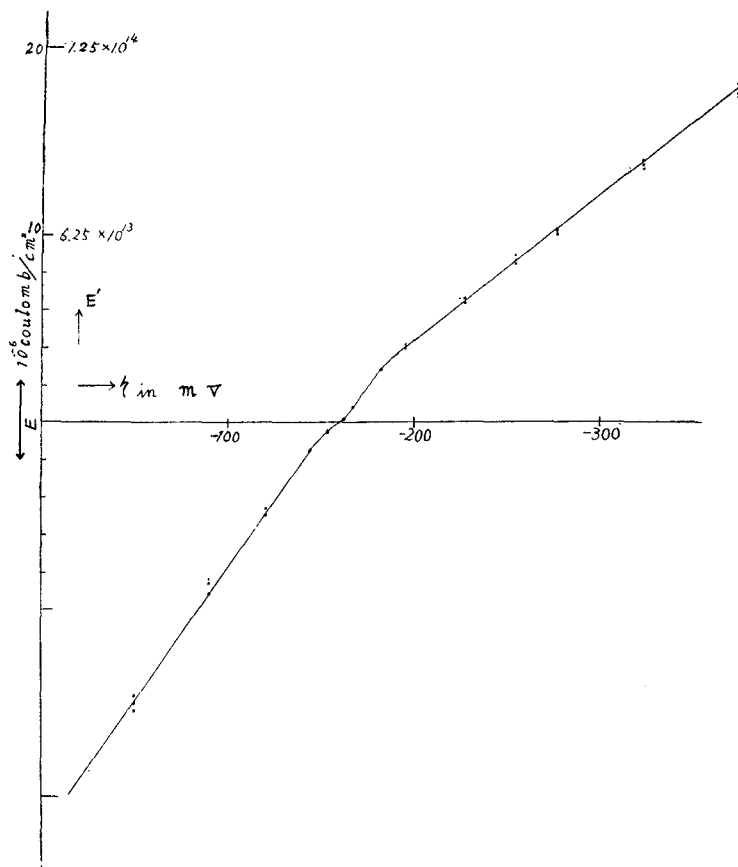


Fig. 15 Electricity required to form unit cathode area.

§ 6. Conclusive remarks

(1) FRUMKIN¹²⁾ objected the authors previous work that platinum colloidal particles formed by the disintegration of the anode may deposit on the mercury cathode surface to mask the genuine hydrogen electrode reaction on mercury.

Assuming that the disintegration of the platinum electrode did occur at all, the contamination of the cathode by these particles should accumulate with time of the electrolysis. The experiment has shown, however, the current density was perfectly reproducible even after the continuation of electrolysis for two months as detailed in §4 and 5. As there exists no reason why the disintegration should occur once for all at the outset, the author is lead to the conclusion that the mercury surface remained uncontaminated in the present experiment.*)

(2) It has been observed that the electrolytic purification of mercury and of aqueous hydrochloric acid in vacuo decreases i and increases E as indicated by the comparison of the present results with earlier ones^{9),13)} of less degree of purification. Recent results, not described

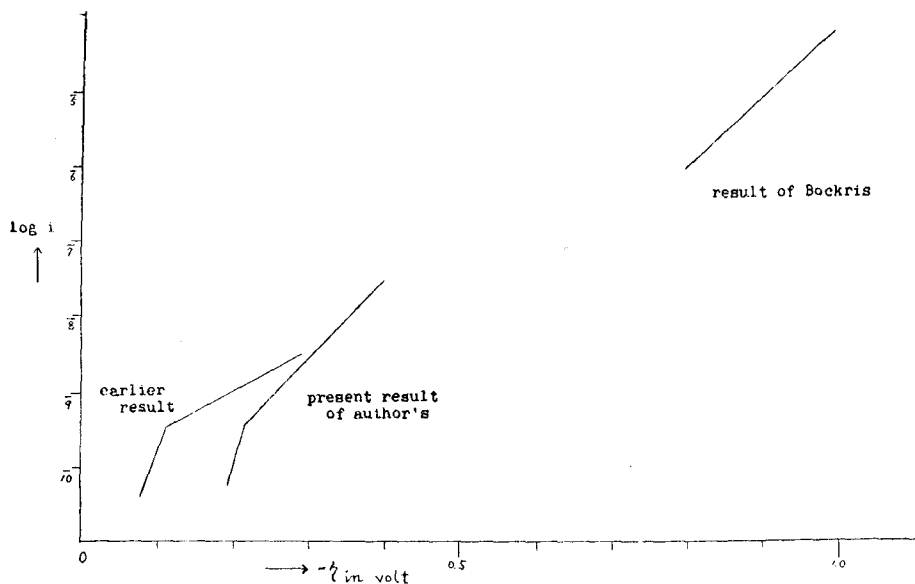


Fig. 16 Comparison of the present result with earlier observations.

*) FRUMKIN himself uses the platinum gauze electrode fitted close above the mercury electrode surface just similarly in the present work. Cf. M. VORSINA and A. FRUMKIN, J. Phys. Chem. USSR 17, 295 (1943).

here, indicate on the other hand that the further purification of the electrode and the electrolyte along the line of scheme of Diagram 1 does not alter the present results. Fig. 16 shows the present results of $\log i-\eta$ -relation in comparison with our earlier results⁸⁾ as well as with that of BÖCKRIS and PARSONS¹¹⁾ at far larger electrode polarization.

The i -value is lower than the earlier result⁸⁾ but still higher than that which would be expected by the linear extrapolation of BÖCKRIS and PARSONS' result.¹¹⁾ Further experiments are going on in this laboratory for investigating the $\log i-\eta$ -relation in the intermediate region.

(3) As seen from Fig. 15, E vanishes at $\eta = -0.160$ volt. This result is in good agreement with the potential at the so-called electrocapillary maximum observed by other workers¹⁵⁾ within experimental errors, but the inclination of E against $-\eta$ or the "capacity" is very much greater both over the higher and lower potentials, i. e., $142 \mu\text{F}/\text{cm}^2$ and $93 \mu\text{F}/\text{cm}^2$, respectively. Recently WAKKAD and SALEM¹⁷⁾ reported that they obtained the value of the capacity of the mercury anodes as $107 \mu\text{F}/\text{cm}^2$ using large surface area and small charging up current densities (of the order of 10^{-7} amp/cm²) in concordance with the present results.

Summary

The relation between the electrode potential η and the current density i on a mercury cathode and also that between η and the electricity E required to create unit surface area of the cathode at high electrode potential were observed.

It was found that there exists a break in the $\log i-\eta$ - as well as in the $E-\eta$ -relation at the same electrode potential, which could be accounted for on the basis of the electrochemical mechanism but not of the slow discharge mechanism.

The author is greatly indebted to Professor J. HORIUTI for his valuable advices and discussions, and it is a pleasure to acknowledge the assistance of Y. KAKIUTI, T. YAMAZAKI, S. HORI and T. AOYAMA of the laboratory.

References

- 1) F. P. BOWDEN and E. K. RIDEAL, *Proc. Roy. Soc. A* **120**, 59 (1928).
- 2) J. HORIUTI and G. OKAMOTO, *Sci. Papers Inst. Phys. Chem. Research (Tokio)* **28**, 1231 (1936).
- 3) B. TOPLEY and H. EYRING, *J. Chem. Physics* **2**, 217 (1934).
- 4) G. OKAMOTO, J. HORIUTI and K. HIROTA, *Sci. Papers Inst. Phys. Chem. Research (Tokio)* **29**, 223 (1936).
- 5) J. HORIUTI, T. KENI and K. HIROTA, *this Journal* **2**, 1 (1951).
- 6) J. HORIUTI, *this Journal* **4**, 55 (1951).
- 7) J. HORIUTI, *this Journal* **1**, 8 (1948).
- 8) J. HORIUTI and A. MITUYA, *this Journal* **2**, 79 (1951).
A. MITUYA, *Bull. Inst. Phys. Chem. Research (Tokio)* **19**, 142 (1940) (in Japanese).
- 9) E. BRUMMER und St. VON NARAY-SZÁBÓ, *Zeit. Elektrochem.* **31**, 95 (1925).
- 10) A. M. AZZAM, J. O'M. BOCKRIS, B. E. CONWAY and H. ROSENBERG, *Trans. Faraday Soc.* **46**, 918 (1950).
- 11) J. HORIUTI and M. IKUSHIMA, *Proc. Imp. Acad. Tokyo* **15**, 39 (1939).
- 12) A. N. FRUMKIN, *Acta Physicochim. U.S.S.R.* **18**, 34 (1943).
- 13) A. MITUYA, T. YAMAZAKI, S. HORI and T. AOYAMA, *Shokubai (Catalyst)*, No. 12, p. 149 (1955) (in Japanese).
- 14) J. O'M. BOCKRIS and R. PARSONS, *Trans. Faraday Soc.* **45**, 916 (1949).
- 15) D. C. GRAHAME, R. P. LARSEN and M. A. POTH, *J. Am. Chem. Soc.* **71**, 2978 (1949).
G. GOUY, *Ann. Phys.* **7**, (9), 129, (1917).
D. C. GRAHAME, *Chem. Rev.* **41**, 441, (1947).
- 16) S. E. S. EL WAKKAD and T. M. SALEM, *J. Chem. Soc.* 1489 (1955).